Ex vivo delivery of regulatory T-cells for control of alloimmune priming in the donor lung

Ei Miyamoto ⓘ, Akihiro Takahagi, Akihiro Ohsumi, Tereza Martinu, David Hwang, Kristen M. Boonstra, Betty Joe, Juan Mauricio Umana, Ke F. Bei, Daniel Vosoughi, Mingyao Liu, Marcelo Cypel, Shaf Keshavjee ⓘ and Stephen C. Juvet ⓘ

Latner Thoracic Surgery Research Laboratories, University Health Network, University of Toronto, Toronto, ON, Canada.

Corresponding author: Stephen C. Juvet (stephen.juvet@uhn.ca)

Abstract

Background Survival after lung transplantation (LTx) is hampered by uncontrolled inflammation and alloimmunity. Regulatory T-cells (Tregs) are being studied as a cellular therapy in solid organ transplantation. Whether these systemically administered Tregs can function at the appropriate location and time is an important concern. We hypothesised that *in vitro*-expanded recipient-derived Tregs can be delivered to donor lungs prior to LTx *via ex vivo* lung perfusion (EVLP), maintaining their immunomodulatory ability.

Methods In a rat model, Wistar Kyoto (WKy) $CD4^+CD25^{high}$ Tregs were expanded *in vitro* prior to EVLP. Expanded Tregs were administered to Fisher 344 (F344) donor lungs during EVLP; left lungs were transplanted into WKy recipients. Treg localisation and function post-transplant were assessed. In a proof-of-concept experiment, cryopreserved expanded human $CD4^+CD25^+CD127^{low}$ Tregs were thawed and injected into discarded human lungs during EVLP.

Results Rat Tregs entered the lung parenchyma and retained suppressive function. Expanded Tregs had no adverse effect on donor lung physiology during EVLP; lung water as measured by wet-to-dry weight ratio was reduced by Treg therapy. The administered cells remained in the graft at 3 days post-transplant where they reduced activation of intra-graft effector $CD4^+$ T-cells; these effects were diminished by day 7. Human Tregs entered the lung parenchyma during EVLP where they expressed key immunoregulatory molecules ($CTLA4^+$, $4\text{-}1BB^+$, $CD39^+$ and $CD15s^+$).

Conclusions Pre-transplant Treg administration can inhibit alloimmunity within the lung allograft at early time points post-transplant. Our organ-directed approach has potential for clinical translation.

Introduction

Lung transplantation (LTx) is life saving in end-stage pulmonary diseases [1]. Unfortunately, despite immunosuppression, median survival after LTx is only 6 years owing to chronic lung allograft dysfunction (CLAD), a syndrome of chronic rejection caused by progressive parenchymal and/or small airway fibrosis. CLAD is driven primarily by recipient alloimmunity, which is augmented by ischaemia-reperfusion injury, infection, air pollution and micro-aspiration. While anti-fibrotic therapies may slow CLAD progression, CLAD prevention by inhibiting alloimmunity is likely to have a greater impact on LTx outcome. Hence, control of the inflammatory tone within the allograft is of paramount importance for preserving long-term lung function in LTx recipients.

$CD4^+CD25^{high}Foxp3^+$ regulatory T-cells (Tregs) can inhibit allograft rejection and are being studied as a systemic cellular therapy in clinical trials of kidney and liver transplantation [2]. Treg therapy for living-donor kidney transplant recipients is safe and feasible, but its efficacy is not established [3]. Although lymphoid organs are a key site of Treg function, a high Treg-to-conventional T-cell (Tconv) ratio

within allografts is required for allograft acceptance [4, 5]. Moreover, lung allografts can be rejected in the absence of secondary lymphoid organs, and the graft is the initial site of alloreactive T-cell priming [6, 7]. Tregs can control alloimmunity within the lung allograft [8], and prior arrival of Tregs may provide even more potent control over Tconv activation than when the cells arrive simultaneously [9, 10]. Thus, post-transplant systemic Treg administration in LTx recipients may not provide timely immune regulation at relevant sites *in vivo*.

We have developed and translated to the bedside a technique of extended *ex vivo* lung perfusion (EVLP) for donor lung assessment and treatment [11] and for gene and cellular therapy delivery in animal and human lungs [12, 13]. Pre-transplant administration of recipient-derived Tregs directly into donor lungs affords the opportunity to seed the allograft with therapeutic immune regulatory cells in advance of the arrival of alloreactive T-cells after graft implantation. Because Tregs can be expanded, cryopreserved and thawed at a later date while retaining function [14], this approach is suitable for LTx from deceased donors.

Here, using a rat model, we tested the hypothesis that *in vitro*-expanded recipient-derived Tregs administered to the donor lung allograft during EVLP prior to transplantation creates an immunoregulatory environment in the lung leading to a diminished anti-donor immune response post-implantation. In a proof-of-concept experiment, we further showed that cryopreserved expanded human Tregs can be delivered successfully to human lungs on EVLP. Our findings have important implications for the use of lung-directed cellular therapies in transplantation and beyond.

Materials and methods

Expanded rat Treg injection during rat EVLP followed by LTx

We opted for a rat model that is amenable to EVLP followed by single LTx, based on prior experience (figure 1a) [15, 16]. We used the Fisher 344 (F344, RT1^{lv})-to-Wistar Kyoto (WKy, RT1^l) strain combination [17]. WKy CD4$^+$CD25^{high} cells were isolated by magnetic and fluorescence-activated cell sorting and expanded with anti-CD3 and anti-CD28 coated beads (Miltenyi Biotec) and 1000 units per mL recombinant human interleukin 2 (rhIL-2) (Chiron) for 7 days. Expanded Tregs were labelled with 5-(and 6-)-(((4-chloromethy)benzoyl)amino)tetramethylrhodamine (CMTMR) (CellTracker Orange, ThermoFisher Scientific) and/or eFluor 450 (eF450) cell proliferation dye (ThermoFisher Scientific) and resuspended in 1 mL Steen solution (XVIVO Perfusion). Normothermic acellular EVLP was performed as previously reported [15]. A total of $4.3–211.3\times10^6$ live Tregs per kg F344 donor body weight were injected into the EVLP circuit upstream of the lungs at 60 min of EVLP. Control grafts received 1 mL Steen containing no cells. Perfusate was sampled upstream and downstream of the lung. At 180 min after injection, the right lung was used for analysis and the left lung was transplanted into a WKy recipient. Recipients were killed at day 3 or 7 post-transplant. The animal study was performed in accordance with the Canadian Council on Animal Care, and the protocol was approved by the Institutional Animal Care Committee (protocol 2853).

Expanded human Treg injection during human EVLP

The human protocol is shown in figure 1b. Healthy donor CD4$^+$CD25$^+$CD127^{low} cells were expanded for 21 days using anti-CD3 and anti-CD28-coated beads (Miltenyi Biotec) and 300 units per mL rhIL-2, and were cryopreserved. Human donor lungs (n=3) on normothermic acellular EVLP and deemed unsuitable for transplantation owing to oedema and/or poor compliance were used. Left or right single lung EVLP was established by clamping the hilum of the worse lung. Cryopreserved Tregs were thawed and labelled with CMTMR and eF450, and a total of $0.4–0.8\times10^9$ were injected in 20 mL Steen into the EVLP circuit upstream of the lung. Tissue samples taken at similar time points from contemporaneous declined lungs undergoing EVLP (no Treg injection, n=5) were obtained as controls. Experiments using human lungs and healthy donor blood were performed in accordance with the Declaration of Helsinki and were approved by the Institutional Research Ethics Board (protocols 06-283 and 17-6229, respectively).

Results

Characteristics of isolated and expanded rat Tregs

We sorted WKy CD4$^+$CD25^{high} cells (highest 2% of CD25$^+$CD4$^+$ T-cells, supplementary figure S1a) and found that they were 73.4±12.8% Foxp3$^+$. Whereas human Tregs are CD4$^+$CD25^{high}CD127^{low}, CD127 and FoxP3 expression were unrelated in rat CD4$^+$ T-cells (not shown). Expansion with anti-CD3 and anti-CD28-coated beads and IL-2 resulted in 152.8±17.1-fold expansion (figure 2a, n=21), with largely retained expression of FoxP3 (63.5±8.3% FoxP3$^+$, supplementary figure S1b) and CD25 (93.6±1.5% CD25$^+$, supplementary figure S1c) at day 7. Tregs upregulated CD8 (81.3±2.4% CD8$^+$, supplementary figure S1d) at day 7, as reported [18]. Expanded Tregs dose-dependently suppressed *in vitro* proliferation of polyclonally stimulated CD4$^+$CD25^{low} Tconv (figure 2b). Beyond 7 days of expansion, the proportion
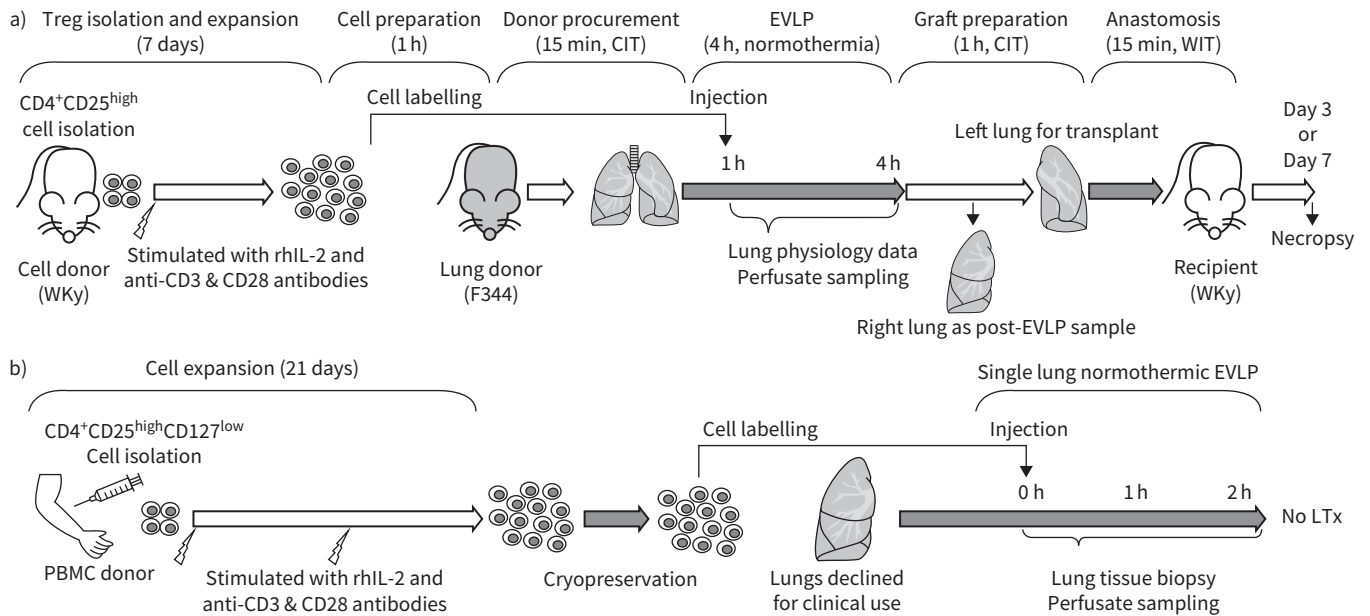
FIGURE 1 Study protocols. a) Schematic of rat regulatory T-cell (Treg) experiment. CD4$^+$CD25^{high} cells (supplementary figure S1a) were isolated from Wistar Kyoto (WKy) rat lymph nodes and expanded with recombinant human interleukin-2 (rhIL-2) and anti-CD3 and anti-CD28 antibodies for 7 days. Prior to starting *ex vivo* lung perfusion (EVLP) with a Fisher 344 (F344) rat heart and lung block, the expanded cells were dye labelled for injection. Labelled Tregs or perfusate vehicle were injected to the circuit at the pulmonary artery port 1 h after the start of EVLP. After 4 h, the left lung graft was transplanted to a WKy recipient while the right lung was subjected to further analyses. b) Schematic of human Treg experiment. CD4$^+$CD25^{high}CD127^{low} cells from a healthy blood donor were isolated and expanded *in vitro*. After 21 days, the expanded Tregs were cryopreserved in liquid nitrogen. Upon notification that a lung was declined for transplantation on EVLP, Tregs were rapidly thawed, labelled with CMTMR and eF450, washed and injected into the EVLP circuit (supplementary figure S6b). EVLP continued for up to 2 h after Treg injection, at which point tissue and perfusate were analysed. CIT: cold ischaemic time; WIT: warm ischaemic time; PBMC: peripheral blood mononuclear cells; LTx: lung transplantation.

of FoxP3$^+$ T-cells decreased (not shown) and so in all rat experiments, cells were used at day 7 of expansion.

Interaction of Tregs with lung allografts during rat EVLP

Tregs were tracked during EVLP (supplementary figure S1f, g) by dye labelling (figure 3a). The proportion of live Tregs rapidly increased in both pulmonary artery and vein perfusate after injection and plateaued within 60 min (figure 3b). Remarkably, ~25% of administered Tregs remained in the EVLP
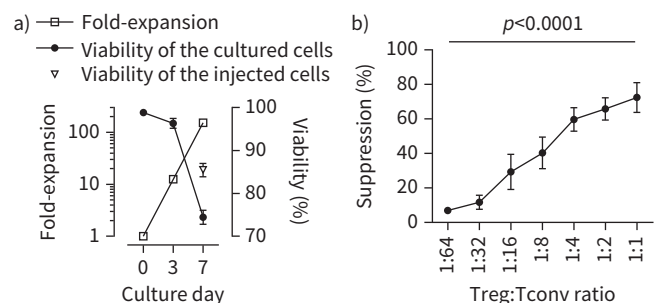

FIGURE 2 *In vitro* expansion of suppressive Wistar Kyoto (WKy) regulatory T-cells (Tregs). a) Treg expansion (n=21). Fold-increase and viability of expanded Tregs on day 3 and day 7 of culture shown. Expanded cells were washed, increasing the viable proportion of injected cells to >80%. b) WKy Tregs mediate dose-dependent suppression of autologous conventional T-cells (Tconv) (n=5, p<0.0001, ANOVA). Gating strategy to identify carboxyfluorescein succinimidyl ester-labelled Tconv is shown in supplementary figure S1c.
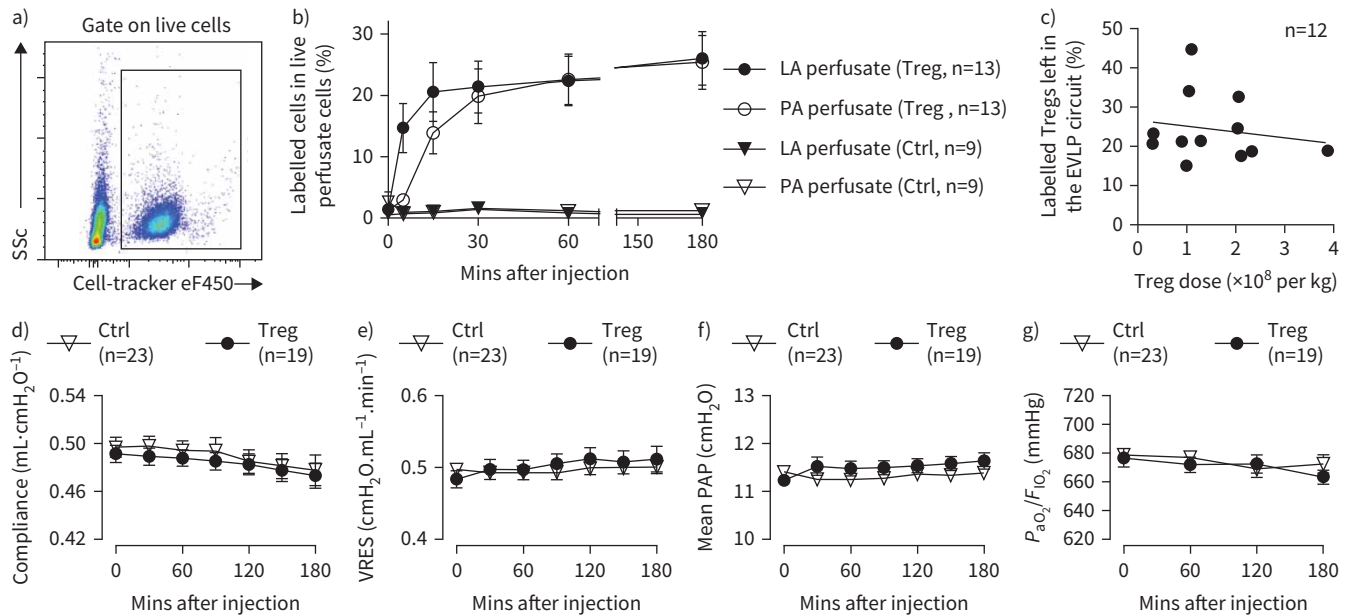
FIGURE 3 Administration of expanded Wistar Kyoto (WKy) regulatory T-cells (Tregs) to allogeneic Fisher 344 (F344) lungs during *ex vivo* lung perfusion (EVLP). a) Identification of labelled Tregs in EVLP perfusate by flow cytometry. SSc: side scatter. b) Proportion of Tregs in live perfusate cells at the pulmonary artery (PA) and left atrium (LA) ports over time, which equalised at 60 min after injection. c) The percentage of Tregs remaining in the circuit at the end of EVLP was calculated as 100×(live cell count in the perfusate)×(fraction of Tregs in live perfusate cells)/ (number of injected cells) (p=0.5886, R^2=0.03028, y= −1.477×X+26.67, linear regression). d) Compliance, e) vascular resistance (VRES) and f) mean pulmonary arterial pressure (PAP) of the donor lungs on EVLP, and g) ratio of the partial pressure of oxygen in the perfusate (P_{aO_2}) to the fraction of inspired oxygen (F_{IO_2}) of allogeneic F344 lungs during EVLP with or without Treg injection. Ctrl: control.

circuit after EVLP regardless of cell dose (figure 3c). Treg infusion did not affect lung compliance (figure 3d), vascular resistance (figure 3e) or mean pulmonary arterial pressure (figure 3f). Gas exchange, measured by the ratio of the arterial partial pressure of oxygen to the fraction of inspired oxygen (figure 3g), and perfusate glucose and lactate concentrations (supplementary figure S2a, b) were unaffected by Treg infusion.

Administered Tregs enter lung allografts and reduce lung vascular permeability at end of EVLP

Acute lung injury scores did not differ between Treg-treated lungs and controls after EVLP (figure 4a and supplementary figure S2c). The wet-to-dry weight ratio was lower in Treg-treated lungs (figure 4b), suggesting that Tregs may have reduced lung oedema; however, zonula occludens-1 (ZO-1) staining, a measure of alveolar tight junction integrity, was similar among Treg-treated lungs and controls (supplementary figure S2d).

After EVLP, CMTMR$^+$ Tregs were seen outside CD31$^+$ vascular structures in the parenchyma (figure 4c). Tregs dose-dependently entered the lung, without evidence of saturation in the range of doses tested (figure 4d). CMTMR$^+$eF450$^+$ Tregs sorted from digested lung tissue at the end of EVLP (supplementary figure S2e) suppressed the proliferation of syngeneic polyclonally stimulated Tconv with a slightly lower potency than Tregs remaining in the EVLP circuit (figure 4e). Compared to control lungs, Treg-treated lungs had higher levels of the Treg-related transcripts forkhead box P3 (FoxP3), cytotoxic T-lymphocyte associated protein 4 (CTLA4), glucocorticoid-induced tumor necrosis factor receptor (GITR) and C-C motif chemokine receptor 4 (CCR4) at the end of EVLP (figure 4f and supplementary figure S2f). There was no difference in the rate of apoptosis, as measured by terminal deoxynucleotidyl transferase dUTP nick end labelling (TUNEL) staining, in Treg-treated lungs up to 200 million Tregs per kg donor body weight, compared to controls (supplementary figure S2g). Further, Tregs themselves were not apoptotic at the end of EVLP (0.97±0.52%, supplementary figure S2h).

Transferred Tregs remain functional in the recipient post-transplant

Transferred Tregs were detectable in the lung at day 3 post-transplant (figure 5a and supplementary figure S3a, b). Compared to the end of EVLP, the cells had shifted to a predominantly subpleural, rather than a
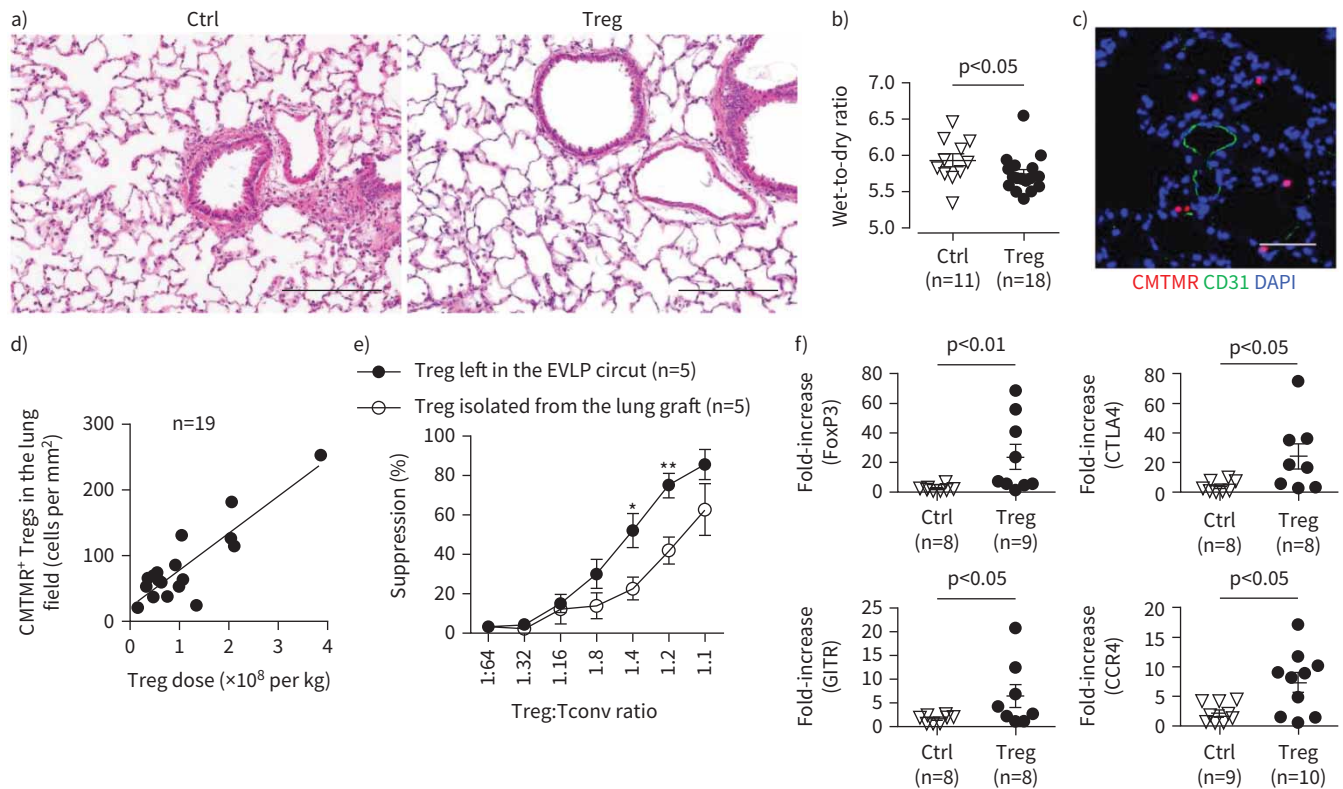
FIGURE 4 Expanded Wistar Kyoto (WKy) regulatory T-cells (Tregs) enter allogeneic Fisher 344 (F344) lungs during *ex vivo* lung perfusion (EVLP) while maintaining their regulatory function and phenotypic properties. a) Representative histology of the lung graft after EVLP (haematoxylin and eosin staining; ×40). Scale bars: 200 μm. b) Wet-to-dry weight ratio in Treg-treated and control (Ctrl) lungs. Control grafts were significantly heavier than Treg-treated ones ($p < 0.05$, Mann–Whitney U test). c) Immunofluorescence staining of the lung graft after EVLP demonstrates $CMTMR^+$ (red) Tregs located in the lung tissue outside $CD31^+$ (green) vessels. Scale bar: 25 μm. d) The number of $CMTMR^+$ cells in the lung parenchyma correlated with the injected dose of Tregs ($p < 0.0001$, $R^2 = 0.7542$, $y = 0.5580x + 22.75$, linear regression). e) Tregs sorted from perfusate (n=5) and digested lung tissue (n=5) at the end of EVLP exhibited dose-dependent suppressive activity toward autologous conventional T-cells (Tconv) ($p = 0.0001$ and $p < 0.0001$ for Tregs isolated from the lung graft and those left in the EVLP circuit, respectively; one-way ANOVA). At a Treg:Tconv ratio of 1:4 and 1:2, Tregs left in the EVLP circuit showed better suppression than those isolated from the lung graft (*: $p < 0.05$; **: $p < 0.01$; two-way repeated-measures ANOVA). f) Treg-related transcripts in the lung graft after EVLP, represented as a fold-increase based on the house-keeping gene. FoxP3, CTLA4, GITR and CCR4 expression were significantly increased in the lung graft of Treg-treated animals compared to control cases. Mann–Whitney U test was applied to compare the groups.

perihilar, location (figure 5b). Tregs mediate contact-dependent modulation of major histocompatibility complex (MHC) class II^+ antigen-presenting cells (APCs) [19]; the percentage of Tregs adjacent to MHC class II^+ cells in the graft was increased on day 3 compared to at the end of EVLP (figure 5c). Further, FoxP3 expression by $CD4^+$ T-cells was higher in Treg-treated allografts than in controls at this time (figure 5d and supplementary figure S3c, d). Untreated lungs exhibited a lesser increase in allograft Treg content at day 3, as has been reported in other transplantation settings [20]. Transferred Tregs were also identified in the draining lymph nodes (dLNs) on day 3, within the extravascular space (figure 5e and supplementary figure S3e).

At day 3 post-transplant, acute lung injury scores did not differ between Treg-treated grafts and controls, with only mild abnormalities in both groups (figure 6a, b and supplementary figure S4a). The number of $CD3^+$ Tconv cells adjacent to MHC class II^+ cells was reduced in Treg-treated lungs compared to controls on day 3 (figure 6c, d). Moreover, within Treg-treated lung allografts, fewer $CD3^+$ Tconv cells were adjacent to MHC class II^+ cells that were closely associated with transferred Tregs in comparison with those that were not (figure 6e).

Treg treatment decreased the percentage of $CD3^+$ T-cells among live cells at day 3 post-transplant (figure 6f and supplementary figure S4c). Upregulation of intercellular adhesion molecule 1 (ICAM1) and CD44 and downregulation of CD62L correlate with rat Tconv activation [21–23]. We observed distinct
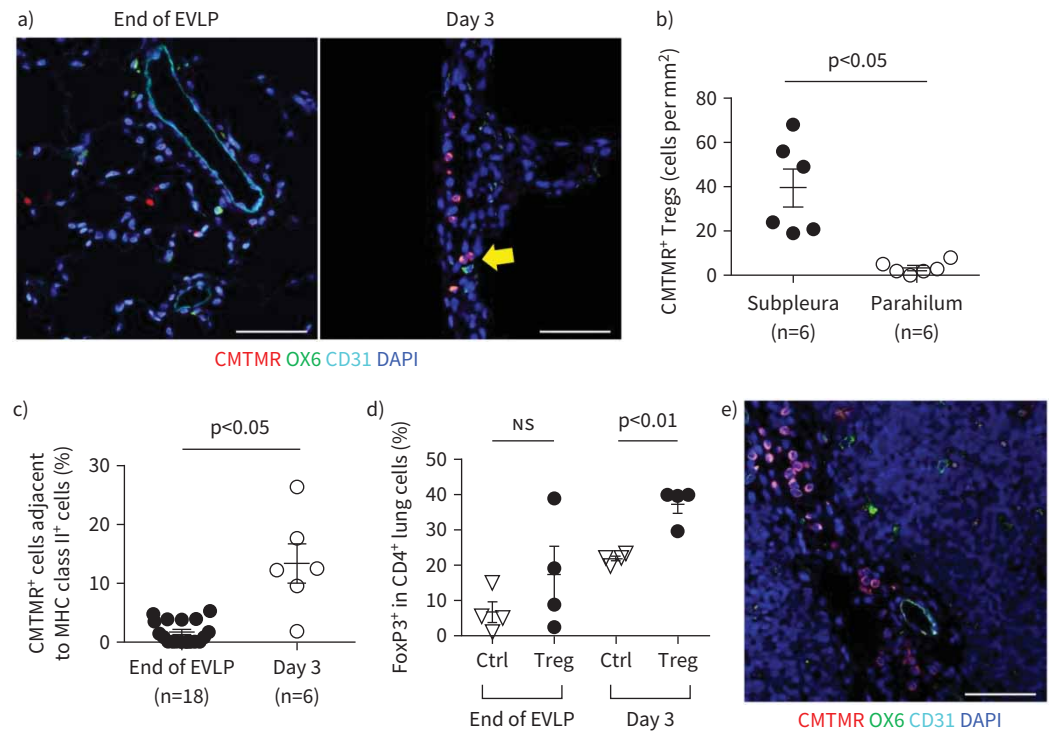
FIGURE 5 Tracking regulatory T-cells (Tregs) in the recipient following lung transplantation (LTx). a) Post-transplant-transferred CMTMR$^+$ Tregs (red) were more predominantly located in the subpleural area (<50 μm from the pleural surface) and more often seen in proximity to major histocompatibility complex (MHC) class II$^+$ (green) cells on day 3 than at the end of *ex vivo* lung perfusion (EVLP) (yellow arrow). Images from each channel are shown in supplementary figure 3a, b. Scale bars: 50 μm. b) Spatial distribution of Tregs in the graft on day 3 (p<0.05, Mann–Whitney U test) and c) increased proximity of Tregs to MHC class II$^+$ cells on day 3 (p<0.05, Mann–Whitney U test). d) The proportion of intra-graft CD4$^+$ T-cells expressing FoxP3 was increased in Treg-treated grafts compared to controls at day 3 post-transplant (p<0.01, Welch's t-test). Gating strategy to identify intra-graft CD4$^+$ T-cells and the representative histograms of FoxP3 expression in them are shown in supplementary figure 3c and d, respectively. n=4 per group. e) Identification of CMTMR$^+$ Tregs (red) in the mediastinal lymph nodes of recipients of Treg-treated lung allografts on day 3. Images from each channel are shown in supplementary figure S3e. Scale bar: 50 μm.

populations of ICAM1$^+$, CD62L$^-$ or CD44$^+$ Tconv in the lungs and dLNs at day 3 (supplementary figure S4d–i). Treg administration during EVLP reduced both the ICAM1$^+$CD44$^+$ subset (figure 6g, h) and the ICAM1$^+$CD62L$^-$ subset (supplementary figure S4j, k) of CD4$^+$ T-cells in the graft and LNs. In contrast, the CD44$^+$CD62L$^-$ subset of CD4$^+$ T-cells was decreased by Treg in the LNs, but not in the lung graft (supplementary figure S4l, m). Treg treatment also decreased ICAM1$^+$CD62L$^-$CD8$^+$ T-cells in the lung graft, but not in the LNs (figure 6i, j). FoxP3 and granzyme B were still elevated compared to controls at day 3 post-transplant in Treg-treated lung grafts (supplementary figure S4n), but not in the dLNs (supplementary figure S4o).

At day 7 post-transplant, acute lung injury and lung allograft rejection scores (International Society for Heart and Lung Transplantation A and B grades) were similar between Treg-treated lungs and controls (supplementary figure S5a, b). CD4$^+$ T-cell numbers were reduced in Treg-treated allografts, although this observation did not reach statistical significance (figure 7a and supplementary figure S5c). Our ability to detect transferred cells at day 7 was impaired, perhaps due to loss of labelling dye. Nevertheless, FoxP3 expression in CD4$^+$ T-cells remained higher in Treg-treated allografts, compared to controls (figure 7b and supplementary figure S5d). CD90 is upregulated on activated rat T-cells [24], and we observed fewer CD90$^+$CD4$^+$ T-cells in the lung allograft at day 7 (figure 7c and supplementary figure S5d); reductions in CD90$^+$CD4$^+$ T-cells were also seen in the dLNs but these findings were not statistically significant. No difference in Treg-related transcripts was observed between Treg-treated lung grafts and controls at day 7 post-transplant (supplementary figure S5e).
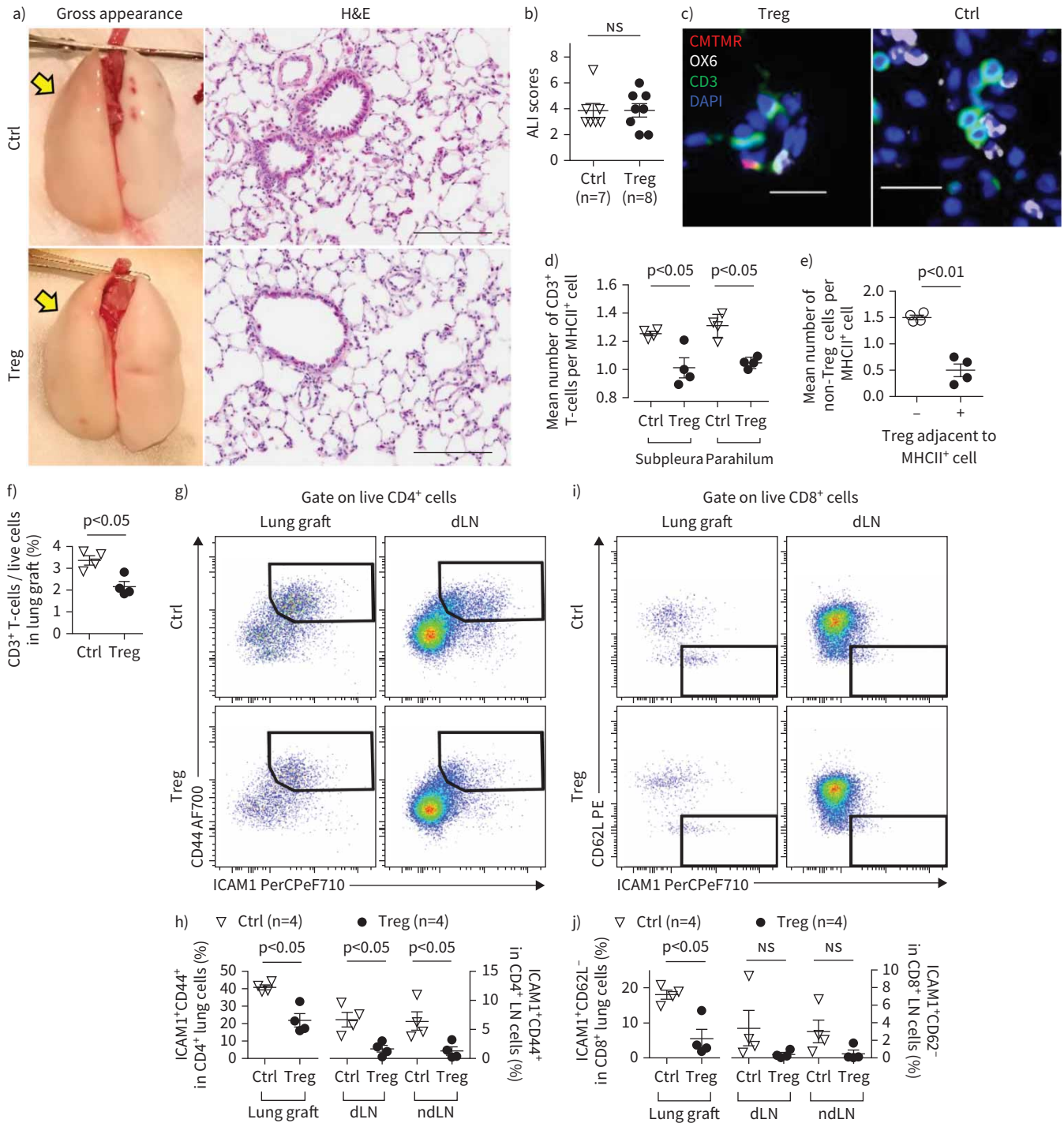
FIGURE 6 Post-transplant immune regulation by expanded regulatory T-cells (Tregs) delivered to the allograft prior to transplantation. a) Representative pictures of the gross appearance and the histology (haematoxylin and eosin (H&E) staining; ×40) of the lung graft (yellow arrows) on day 3 post-transplant. Scale bars: 200 µm. b) Acute lung injury (ALI) scores (0–12) in Treg-treated and control (Ctrl) grafts. Details of histological semi-quantification are shown in supplementary figure S4a. c) Representative high power immunofluorescence images showing intra-graft major histocompatibility complex (MHC) class II$^+$ cells (white) adjacent to CMTMR$^-$CD3$^+$ non-transferred conventional T-cells (Tconv) (green) and CMTMR$^+$CD3$^+$ transferred Tregs (red). Scale bars: 20 µm. d) Mean number of CD3$^+$ T-cells adjacent to MHC class II$^+$ cells in at least 10 high powered fields in Treg-treated and control lungs at the subpleural and perihilar areas. n=4 per group. e) Number of Tconv adjacent to MHC class II$^+$ cells without (−) or with (+) an adjacent Treg cell (paired t-test applied). n=4 per group. f) The percentage of CD3$^+$ T-cells (gating strategy shown in supplementary figure 4b), as well as CD4$^+$ T-cells and CD8$^+$ T-cells (supplementary figure S4c), was significantly decreased in Treg-treated lung graft on day 3. g) Flow cytometric analysis of CD44 and ICAM1 expression on CD4$^+$ cells from the lung allograft and draining lymph node (dLN).

h) Percentage of ICAM1^{+}CD44^{+} cells in the CD4^{+} T-cell compartment in the lung, dLN and non-draining lymph node (ndLN) at day 3. i) Flow cytometric analysis of CD62L and ICAM1 expression on CD8^{+} cells from the lung allograft and dLN. j) Percentage of ICAM1^{+}CD62L^{−} cells in the CD8^{+} T-cell compartment in the lung, dLN and dLN at day 3. Mann–Whitney U test was applied to compare the groups unless otherwise specified. NS: nonsignificant.

Administration of allogeneic human Tregs during human EVLP

Human Tregs expanded 1067.7±363.4-fold and were 96.3±1.2% viable after 21 days in culture (supplementary table S1). Viable cells were 81.4±4.7% FoxP3^{+} and 81.8±5.3% CTLA4^{+} (figure 8a). Lung donor characteristics and EVLP parameters are shown in supplementary table S2. Injected Tregs were 87.1±1.2% viable and 80.2±6.7% CD4^{+}CD127^{low}. EVLP perfusate measurements are shown in supplementary table S1. Transferred Tregs were identifiable in perfusate and lung tissue samples obtained 1 h after injection (figure 8b, c and supplementary figure S6c). Expression of key functional Treg markers CTLA4, CD15s, CD39, 4-1BB and CXCR4 was higher in lung than in perfusate Tregs 1 h after injection (figure 8d). CCR4 expression was also higher in lung than in perfusate Tregs, although this observation was not statistically significant (figure 8d). Further, although lung Tregs exhibited higher CD40L and CD45RA expression, there was no clear difference in the expression of FoxP3 or several other Treg- and chemokine-related molecules (supplementary figure S6d). In lung tissue, Treg-related transcripts IL-10, granzyme B and indoleamine 2,3-dioxygenase 1 (IDO-1) increased 1 h after Treg injection compared to controls over a similar period on EVLP (figure 8e). Interestingly, FoxP3 and CTLA4 were not consistently upregulated in Treg-treated lungs compared to controls (supplementary figure S6e).

Discussion

EVLP assessment of graft function prior to LTx has expanded the donor pool, with short- and long-term outcomes equivalent to conventional LTx [25]. EVLP also holds promise as a tool for delivering advanced cell and gene therapies to reduce lung allograft injury [12, 26]. Furthermore, it provides an opportunity to immunologically manipulate the donor organ in the recipient's favour prior to the arrival of recipient
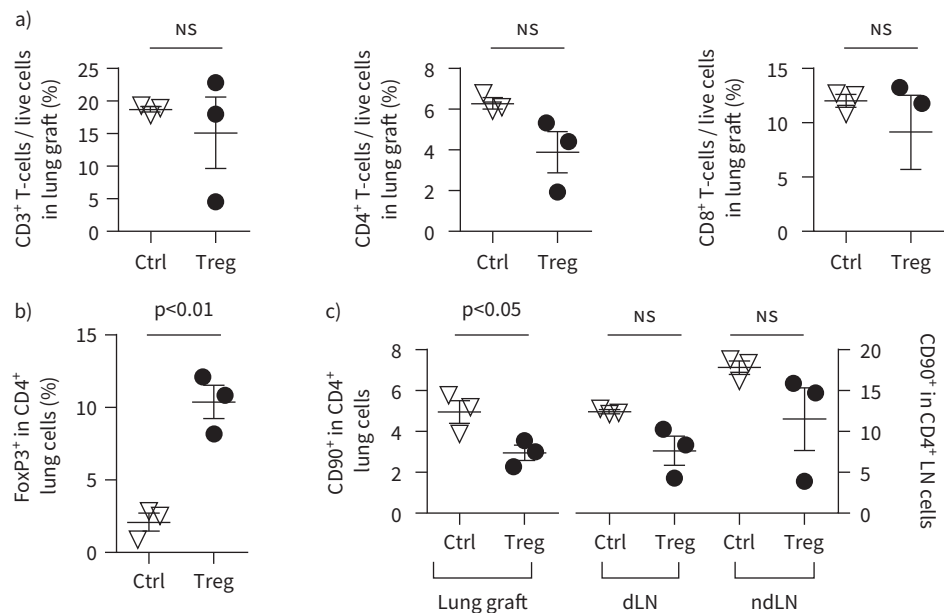

FIGURE 7 Suboptimal control of conventional T-cell (Tconv) response in the lung at 7 days post-transplant. a) Percentage of T-cells in regulatory T-cell (Treg)-treated lung graft on day 7. Gating strategy is shown in supplementary figure S5c. n=3 per group. b) Percentage of FoxP3^{+} in CD4^{+} T-cells was significantly increased in Treg-treated lung graft on day 7, compared to control (Ctrl) lungs. n=3 per group. c) CD90 expression on CD4^{+} T-cells was significantly decreased in the lung graft of Treg-treated animals compared to control cases, but not statistically significant in draining lymph nodes (dLN) and non-draining lymph nodes (ndLN). n=3 per group. Analysis of FoxP3 and CD90 expression in CD4^{+} T-cells is shown in supplementary figure S5d. Mann–Whitney U test was applied to compare the groups. NS: nonsignificant.
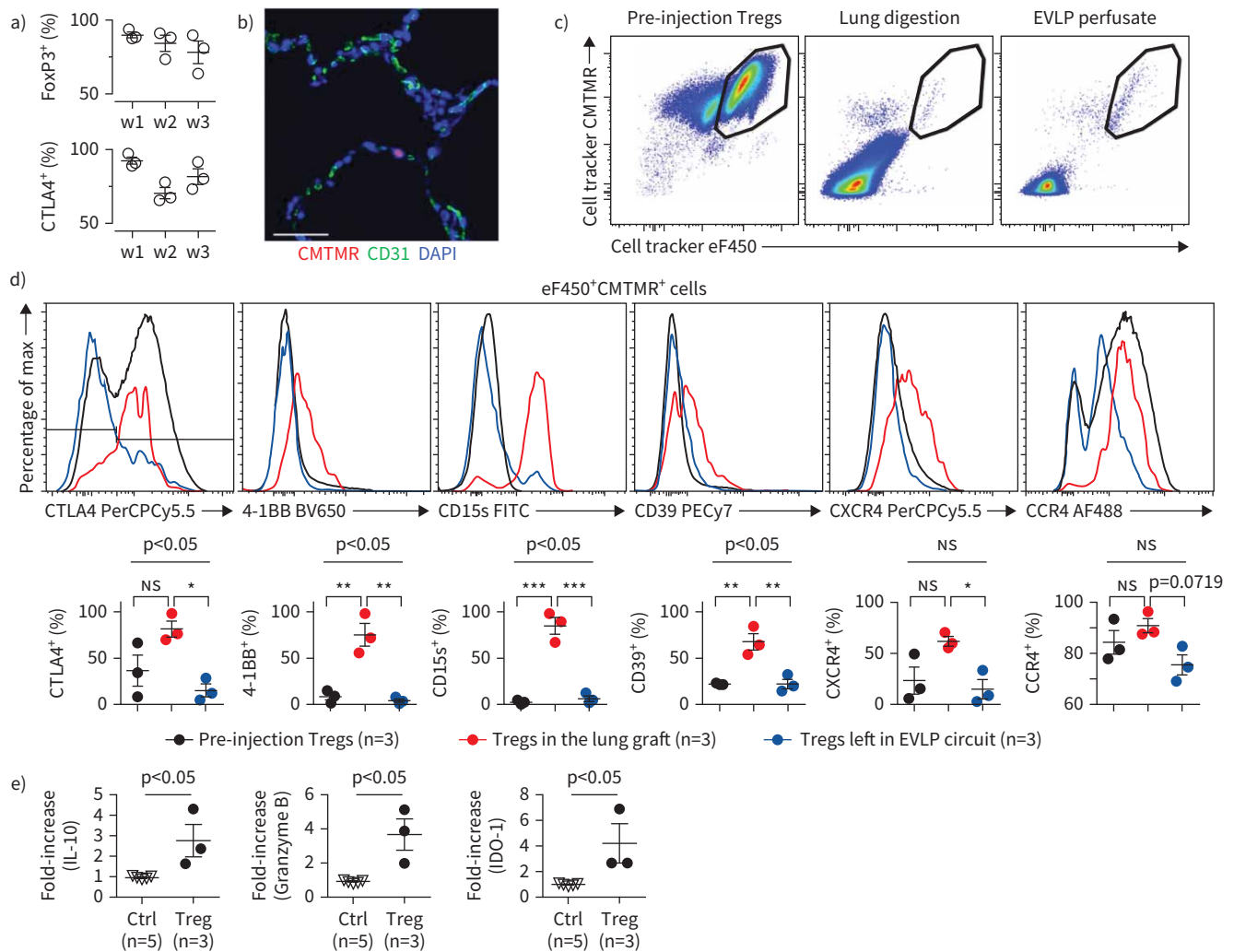
FIGURE 8 Delivery of human regulatory T-cells (Tregs) to allogeneic human lungs during *ex vivo* lung perfusion (EVLP). a) Expression of FoxP3 and CTLA4 during 21 days of expansion. n=3 per group. b) Immunofluorescence staining of the lung graft 1 h after Treg administration. CMTMR$^+$ cells (red) were identifiable in the parenchyma. Images from each channel are shown in supplementary figure 6c. Scale bar: 50 µm. c) Flow cytometric analysis of Tregs before injection (left panel), in the lung graft (middle panel) and in the perfusate (right panel) 1 h after injection. d) Analysis of the expression of the indicated markers on eF450$^+$CMTMR$^+$ cells prior to injection (black lines), in the perfusate (blue lines) and in the lung allograft (red lines) 1 h after injection, and those left in the EVLP circuit. n=3 per group. Repeated measures one-way ANOVA revealed that there were significant differences in the expression of CTLA4, 4-1BB, CD15s and CD39 on Tregs between the groups. The expression of CXCR4 (p=0.0339) and CCR4 (p=0.0719) was higher in Tregs in the lung graft than in those left in the EVLP circuit (Tukey's test), although the intergroup difference was not significant. The majority of Tregs in the lung graft were positive for CCR4 (90.9±2.8%). NS: nonsignificant; *: p<0.05; **: p<0.01; ***: p<0.001 (Tukey's test). e) Quantitative PCR analysis of the indicated transcripts in lung tissue. Transcripts measured at the end of EVLP and normalised to the housekeeping gene *PPIA* are displayed as a ratio to their abundance at the beginning of EVLP. Results from Treg-treated lungs (n=3) are compared to results from untreated contemporaneous discarded lungs at the beginning and end of EVLP (n=5). Mann–Whitney U tests, p<0.05 for IL-10, granzyme B and IDO-1.

leukocytes. With this concept in mind, we used EVLP to examine whether pre-transplant administration of expanded recipient Tregs to the graft could modify the alloimmune response at its earliest stages.

We successfully expanded suppressive rat CD4$^+$CD25^{high} Tregs with properties comparable to mouse and human Tregs [27, 28]. The cells were not harmful across a wide range of doses; ~25% of the administered cells remained in the EVLP circuit irrespective of dose. Chemokine receptors can promote Treg entry into tissues [29]. We found that CXCR4, but not CCR5, CCD6, CCR7 or CXCR3, were more highly expressed in Tregs entering human lungs than in those remaining in the EVLP circuit. CCR4 expression was also higher in lung than in perfusate Tregs, and although this finding was not statistically significant, the rat and

human data collectively suggest that CXCR4 and CCR4 may be involved in migration of the cells into the lung. While the T-cell receptor (TCR)–MHC interaction mediates CD8$^+$ T-cell uptake by allografts [30], its role in CD4$^+$ T-cell uptake is less clear [31, 32]. Moreover, only ∼5–15% of T-cells are alloreactive [33–36], suggesting that Treg uptake is not strictly TCR-dependent. The roles of chemokine receptors and the TCR in Treg entry to lung allografts remain uncertain and will require further study.

Tregs entered the parenchyma without causing injury. Movement of water out of pulmonary capillaries into the interstitium and alveolar spaces contributes to lung injury and primary graft dysfunction following LTx [37, 38]. Typically, the alveolar–capillary barrier is disrupted, which can be revealed by ZO-1 staining [12]. Although lung water was reduced in Treg-treated lungs compared with controls, ZO-1 staining was not altered at the end of EVLP despite our prediction that Tregs might have promoted improved alveolar–capillary barrier integrity. The degree of injury in these lungs may have been too mild to detect meaningful differences, given that the wet-to-dry weight ratio of control lungs was also near normal [39]. It is conceivable that Tregs may have altered one or more physiological alveolar fluid clearance pathways [40]. Whether polyclonally expanded Tregs can repair damaged lungs is an important question that awaits further investigation.

Intra-graft immune regulatory transcripts were increased after Treg infusion in the rat (FoxP3, CTLA4, CCR4 and GITR) and human (IL-10 and IDO-1) models, and Tregs sorted from treated rat lungs retained suppressive function, although with lower potency than Tregs remaining in the perfusate. This difference might reflect reduced viability or loss of functional molecules caused by enzymatic digestion, or indicate that Tregs entering the lung were intrinsically less functional. Nevertheless, they continued to exert immune regulation *in vivo* post-transplant. At day 3, they exhibited increased proximity to APCs, the principal site of immune regulation by Tregs *in vivo* [19]. Recipient Tconv, in contrast, displayed reduced proximity to APCs in the presence of Tregs, with Treg-associated APCs showing the lowest proximity to Tconv. Further, Tconv in Treg-treated lungs and dLNs exhibited reduced T-cell activation marker expression compared to controls. These are important findings, because lung allograft CD11c$^+$ APCs are the initial site of T-cell priming, which has already occurred by day 3 post-transplant [6]. Collectively, these data support the concept of pre-transplant Treg delivery to the organ.

For polyclonal Treg therapies, such as the ones used here, it is estimated that a 1:1 or 1:2 Treg:Tconv ratio is required within the target organ to inhibit rejection [41]. To achieve this ratio with systemic Treg administration might be difficult, but our approach boosted the Treg:Tconv ratio in the graft from 1:5 up to 1:2 at 3 days post-transplant (figure 5d), suggesting a means by which to attain this goal.

Transplanted lungs are directly exposed to the external environment *via* the airways, rendering them susceptible to inflammatory stimuli that enhance risks for rejection and CLAD [42–44]. Intra-graft immune regulatory mechanisms are therefore likely to be even more important in LTx than in other transplanted organs. While our approach resulted in ∼40% of CD4$^+$ T-cells expressing FoxP3 at day 3 post-LTx (figure 5d), only ∼10% expressed FoxP3 at day 7 (figure 7d), which may explain why we did not observe an impact on acute rejection at day 7. Indeed, lung allograft residency by Tregs is likely to be required for lung allograft acceptance [45], and we speculate that ongoing engagement of peripheral tolerance mechanisms in the graft will be needed to prevent rejection after LTx.

Our study has several limitations. Only a minority of polyclonal Tregs are reactive to donor antigens, and further, we cannot be certain that the reduced Tconv activation seen in the presence of Tregs was strictly due to control of the alloimmune response, given that we did not assess these phenomena in a syngeneic control group. Ultimately, because donor antigen-reactive Tregs are more potent than polyclonal Tregs [46], it would be desirable to combine our approach with chimeric antigen receptors [47, 48]. We did not administer immunosuppressive drugs and because calcineurin inhibitors can limit Treg function [49], it is likely that standard LTx immunosuppression would reduce effectiveness. We did not evaluate the resistance of the Tregs to conversion to harmful effector cells; however, we used naturally occurring (originating in the thymus) Tregs in our study, which are more stable than *in vitro*-induced Tregs [45]. Future work will be needed to evaluate Treg stability in this context. We were unable to track administered cells beyond day 3, perhaps due to dilution of labelling dyes and/or cell death or migration; nevertheless, FoxP3$^+$ cells were more prevalent among CD4$^+$ T-cells in Treg-treated grafts than in controls at 7 days post-transplant. Selective immunosuppressive approaches to enhance Treg responses are emerging [50, 51] and it would be attractive to combine one of them with pre-transplant Treg administration.

In summary, recipient-derived expanded Tregs can be administered to rat and human lungs during EVLP. The cells did not injure the grafts and inhibited Tconv responses *in vitro* and *in vivo*. Our findings

therefore support the concept that immune modulation can begin in the allograft prior to transplantation, opening the door to personalised organ-directed immunoregulatory cell therapy.

References

1   Yusen RD, Edwards LB, Dipchand AI, *et al.* The Registry of the International Society for Heart and Lung Transplantation: thirty-third adult lung and heart–lung transplant report—2016; focus theme: primary diagnostic indications for transplant. *J Heart Lung Transplant* 2016; 35: 1170–1184.

2   Vaikunthanathan T, Safinia N, Boardman D, *et al.* Regulatory T cells: tolerance induction in solid organ transplantation. *Clin Exp Immunol* 2017; 189: 197–210.

3   Sawitzki B, Harden PN, Reinke P, *et al.* Regulatory cell therapy in kidney transplantation (the ONE study): a harmonised design and analysis of seven non-randomised, single-arm, phase 1/2A trials. *Lancet* 2020; 395: 1627–1639.

4   Young JS, Yin D, Vannier AGL, *et al.* Equal expansion of endogenous transplant-specific regulatory T cell and recruitment into the allograft during rejection and tolerance. *Front Immunol* 2018; 9: 1385.

5   Graca L, Cobbold SP, Waldmann H. Identification of regulatory T cells in tolerated allografts. *J Exp Med* 2002; 195: 1641–1646.

6   Gelman AE, Li W, Richardson SB, *et al.* Acute lung allograft rejection is independent of secondary lymphoid organs. *J Immunol* 2009; 182: 3969–3973.

7   Wagnetz D, Sato M, Hirayama S, *et al.* Rejection of tracheal allograft by intrapulmonary lymphoid neogenesis in the absence of secondary lymphoid organs. *Transplantation* 2012; 93: 1212–1220.

8   Li W, Gauthier JM, Tong AY, *et al.* Lymphatic drainage from bronchus-associated lymphoid tissue in tolerant lung allografts promotes peripheral tolerance. *J Clin Invest* 2020; 130: 6718–6727.

9   Nguyen VH, Zeiser R, DaSilva DL, *et al. In vivo* dynamics of regulatory T-cell trafficking and survival predict effective strategies to control graft-*versus*-host disease following allogeneic transplantation. *Blood* 2007; 109: 2649–2656.

10   Zhang P, Tey S-KK, Koyama M, *et al.* Induced regulatory T cells promote tolerance when stabilized by rapamycin and IL-2 *in vivo. J Immunol* 2013; 191: 5291–5303.

11 Cypel M, Yeung JC, Mingyao L, *et al.* Normothermic *ex vivo* lung perfusion in clinical lung transplantation. *N Engl J Med* 2011; 364: 1431–1440.

12 Cypel M, Liu M, Rubacha M, *et al.* Functional repair of human donor lungs by IL-10 gene therapy. *Sci Transl Med* 2009; 1: 4ra9.

13 Mordant P, Nakajima D, Kalaf R, *et al.* Mesenchymal stem cell treatment is associated with decreased perfusate concentration of interleukin-8 during *ex vivo* perfusion of donor lungs after 18-hour preservation. *J Heart Lung Transplant* 2016; 35: 1245–1254.

14 Nadig SN, Wickiewicz J, Wu DC, *et al. In vivo* prevention of transplant arteriosclerosis by *ex vivo*-expanded human regulatory T cells. *Nat Med* 2010; 16: 809–813.

15 Ohsumi A, Kanou T, Ali A, *et al.* A method for translational rat *ex vivo* lung perfusion experimentation. *Am J Physiol Lung Cell Mol Physiol* 2020; 319: L61–L70.

16 Noda K, Tane S, Haam SJ, *et al.* Optimal *ex vivo* lung perfusion techniques with oxygenated perfusate. *J Heart Lung Transplant* 2017; 36: 466–474.

17 Von Süßkind-Schwendi M, Ruemmele P, Schmid C, *et al.* Lung transplantation in the Fischer 344-Wistar Kyoto strain combination is a relevant experimental model to study the development of bronchiolitis obliterans in the rat. *Exp Lung Res* 2012; 38: 111–123.

18 Verma ND, Robinson CM, Carter N, *et al.* Alloactivation of naïve CD4^{+} CD8^{−} CD25^{+} T regulatory cells: expression of CD8α identifies potent suppressor cells that can promote transplant tolerance induction. *Front Immunol* 2019; 10: 2397.

19 Tang Q, Adams JY, Tooley AJ, *et al.* Visualizing regulatory T-cell control of autoimmune responses in nonobese diabetic mice. *Nat Immunol* 2006; 7: 83–92.

20 Fan Z, Spencer JA, Lu Y, *et al. In vivo* tracking of "color-coded" effector, natural and induced regulatory T cells in the allograft response. *Nat Med* 2010; 16: 718–722.

21 Mesri M, Liversidge J, Forrester J V. ICAM-1/LFA-1 interactions in T-lymphocyte activation and adhesion to cells of the blood–retina barrier in the rat. *Immunology* 1994; 83: 52–57.

22 Ponta H, Sherman L, Herrlich PA. CD44: from adhesion molecules to signalling regulators. *Nat Rev Mol Cell Biol* 2003; 4: 33–45.

23 Hengel RL, Thaker V, Pavlick M V, *et al.* Cutting edge: L-selectin (CD62L) expression distinguishes small resting memory CD4^{+} T cells that preferentially respond to recall antigen. *J Immunol* 2003; 170: 28–32.

24 Paterson DJ, Jefferies WA, Green JR, *et al.* Antigens of activated rat T lymphocytes including a molecule of 50,000 Mr detected only on CD4 positive T blasts. *Mol Immunol* 1987; 24: 1281–1290.

25 Yeung JC, Krueger T, Yasufuku K, *et al.* Outcomes after transplantation of lungs preserved for more than 12 h: a retrospective study. *Lancet Respir Med* 2017; 5: 119–124.

26 Nakajima D, Watanabe Y, Ohsumi A, *et al.* Mesenchymal stromal cell therapy during *ex vivo* lung perfusion ameliorates ischemia-reperfusion injury in lung transplantation. *J Heart Lung Transplant* 2019; 38: 1214–1223.

27 Ward ST, Li KK, Curbishley SM. A method for conducting suppression assays using small numbers of tissue-isolated regulatory T cells. *MethodsX* 2014; 1: 168–174.

28 Mcmurchy AN, Levings MK. Suppression assays with human T regulatory cells: a technical guide. *Eur J Immunol* 2012; 42: 27–34.

29 Liston A, Gray DHD. Homeostatic control of regulatory T cell diversity. *Nat Rev Immunol* 2014; 14: 154–165.

30 Walch JM, Zeng Q, Li Q, *et al.* Cognate antigen directs CD8^{+} T-cell migration to vascularized transplants. *J Clin Invest* 2013; 123: 2663–2671.

31 Krupnick AS, Gelman AE, Barchet W, *et al.* Cutting edge: murine vascular endothelium activates and induces the generation of allogeneic CD4^{+} 25^{+} Foxp3^{+} regulatory T cells. *J Immunol* 2005; 175: 6265–6270.

32 Kreisel D, Krasinskas AM, Krupnick AS, *et al.* Vascular endothelium does not activate CD4^{+} direct allorecognition in graft rejection. *J Immunol* 2004; 173: 3027–3034.

33 Noorchashm H, Lieu YK, Rostami SY, *et al.* A direct method for the calculation of alloreactive CD4^{+} T-cell precursor frequency. *Transplantation* 1999; 67: 1281–1284.

34 Lalfer M, Chappert P, Carpentier M, *et al.* Foxp3^{+} regulatory and conventional CD4^{+} T-cells display similarly high frequencies of alloantigen-reactive cells. *Front Immunol* 2019; 10: 1.

35 Suchin EJ, Langmuir PB, Palmer E, *et al.* Quantifying the frequency of alloreactive T-cells *in vivo*: new answers to an old question. *J Immunol* 2001; 166: 973–981.

36 Juvet SC, Sanderson S, Hester J, *et al.* Quantification of CD4^{+}T-cell alloreactivity and its control by regulatory T-cells using time-lapse microscopy and immune synapse detection. *Am J Transplant* 2016; 16: 1394–1407.

37 Pottecher J, Roche AC, Dégot T, *et al.* Increased extravascular lung water and plasma biomarkers of acute lung injury precede oxygenation impairment in primary graft dysfunction after lung transplantation. *Transplantation* 2017; 101: 112–121.

38 Trebbia G, Sage E, Le Guen M, *et al.* Assessment of lung edema during *ex vivo* lung perfusion by single transpulmonary thermodilution: a preliminary study in humans. *J Heart Lung Transplant* 2019; 38: 83–91.

39 Kondo T, Chen F, Ohsumi A, *et al.* β2-adrenoreceptor agonist inhalation during *ex vivo* lung perfusion attenuates lung injury. *Ann Thorac Surg* 2015; 100: 480–486.

40   Huppert LA, Matthay MA. Alveolar fluid clearance in pathologically relevant conditions: *in vitro* and *in vivo* models of acute respiratory distress syndrome. *Front Immunol* 2017; 8: 371.

41   Tang Q, Lee K. Regulatory T-cell therapy for transplantation: how many cells do we need? *Curr Opin Organ Transplant* 2012; 17: 349–354.

42   Verleden GM, Glanville AR, Lease ED, *et al.* Chronic lung allograft dysfunction: definition, diagnostic criteria, and approaches to treatment—a consensus report from the Pulmonary Council of the ISHLT. *J Heart Lung Transplant* 2019; 38: 493–503.

43   Belperio JA, Weigt SS, Fishbein MC, *et al.* Chronic lung allograft rejection: mechanisms and therapy. *Proc Am Thorac Soc* 2009; 6: 108–121.

44   Husain AN, Siddiqui MT, Holmes EW, *et al.* Analysis of risk factors for the development of bronchiolitis obliterans syndrome. *Am J Respir Crit Care Med* 1995; 159: 829–833.

45   Li W, Gauthier JM, Higashikubo R, *et al.* Bronchus-associated lymphoid tissue–resident Foxp3^{+} T lymphocytes prevent antibody-mediated lung rejection. *J Clin Invest* 2019; 129: 556–568.

46   Sagoo P, Ali N, Garg G, *et al.* Human regulatory T-cells with alloantigen specificity are more potent inhibitors of alloimmune skin graft damage than polyclonal regulatory T-cells. *Sci Transl Med* 2011; 3: 83ra42.

47   MacDonald KG, Hoeppli RE, Huang Q, *et al.* Alloantigen-specific regulatory T-cells generated with a chimeric antigen receptor. *J Clin Invest* 2016; 126: 1413–1424.

48   Noyan F, Zimmermann K, Hardtke-Wolenski M, *et al.* Prevention of allograft rejection by use of regulatory T-cells with an MHC-specific chimeric antigen receptor. *Am J Transplant* 2017; 17: 917–930.

49   Akimova T, Kamath BM, Goebel JW, *et al.* Differing effects of rapamycin or calcineurin inhibitor on T-regulatory cells in pediatric liver and kidney transplant recipients. *Am J Transplant* 2012; 12: 3449–3461.

50   Whitehouse G, Gray E, Mastoridis S, *et al.* IL-2 therapy restores regulatory T-cell dysfunction induced by calcineurin inhibitors. *Proc Natl Acad Sci USA* 2017; 114: 7083–7088.

51   Sockolosky JT, Trotta E, Parisi G, *et al.* Selective targeting of engineered T-cells using orthogonal IL-2 cytokine-receptor complexes. *Science* 2018; 359: 1037–1042.